COMMUNICATION

Architecture of β-Graphdiyne-Containing Thin Film Using Modified Glaser–Hay Coupling Reaction for Enhanced Photocatalytic Property of TiO_2

Jiaqiang Li, Ziqian Xie, Yan Xiong, Zhenzhu Li, Qunxing Huang, Shuqing Zhang, Jingyuan Zhou, Rong Liu, Xin Gao, Changguo Chen, Lianming Tong, Jin Zhang,* and Zhongfan Liu**

β-Graphdiyne (β-GDY) is a member of 2D graphyne family with zero band gap, and is a promising material with potential applications in energy storage, organic electronics, etc. However, the synthesis of β-GDY has not been realized yet, and the measurement of its intrinsic properties remains elusive. In this work, β-GDY-containing thin film is successfully synthesized on copper foil using modified Glaser–Hay coupling reaction with tetraethynylethene as precursor. The as-grown carbon film has a smooth surface and is continuous and uniform. Electrical measurements reveal the conductivity of 3.47×10^{-6} S m^{-1} and the work function of 5.22 eV. TiO_2@β-GDY nanocomposite is then prepared and presented with an enhancement of photocatalytic ability compared to pure TiO_2.

The extensive properties and applications of carbon materials depend on the hybridization of carbon atoms, namely, sp, sp^2, or sp^3.[1] Since the Nobel-Prize-winning discovery of buckminsterfullerene C60,[2] tremendous efforts have been devoted to develop new carbon allotropes, such as carbon nanotubes and graphene, which possess extraordinary electrical, mechanical, and optical properties, leading to diverse advanced applications.[3,4] In 1987, Baughman first proposed another kind of 2D carbon allotrope, graphyne (GY), which only contains sp and sp^2 hybridized carbon atoms.[5] The presence of acetylenic groups in GY introduces a variety of optical and electronic properties that are quite different from graphene and carbon nanotubes.[6] However, the synthesis of a novel and stable form of GY still remains elusive.

Graphdiyne (GDY), another member of 2D graphyne family, can be described as GY networks, where all acetylenic (−C≡C−) linkages are replaced by diacetylenic linkages (−C≡C−C≡C−) that are synthetically approachable.[5,7] According to the different arrangement of carbon atoms, GDY could be mainly divided into three forms, namely, α-, β-, and γ-GDY (Figure S1, Supporting Information).[8] In 2010, Li and coworkers have successfully synthesized γ-GDY on copper substrates through acetylenic coupling reaction using hexakisethynylbenzene as precursor.[9] γ-GDY has been predicted to be the most stable structure among the three forms with a band gap of ≈0.46 eV and own unique anisotropic properties.[7] These advantages make γ-GDY promising for various applications.[10–24]

Different from γ-GDY, β-GDY is a zero band gap material and presents a metallic behavior like graphene.[8,25] It contains two-diacetylenic linkages (−C≡C−C≡C−) between two sp^2 carbon atoms of ethylene to form a carbon network with uniformly distributed pore structure.[26] Besides its triangular geometries, β-GDY also has hexagonal geometries, which means larger pore size and lower planer packing density compared to γ-GDY.[8] These advantages make β-GDY a promising material to be applied as selective membranes for molecular sieves, lithium or hydrogen storage, heterogeneous catalysis, and electronic chemistry.[27] Calculations of the electronic structure reveal the existence of Dirac points, leading to the intrinsic carry mobility of β-GDY as high as graphene.[28] Dirac point movement study under rotating uniaxial and shear strains indicates that β-GDY presents strong anisotropy.[29] Furthermore, β-GDY has higher percentage of acetylenic linkages (67%) than γ-GDY (50%), meaning stronger π-conjunction compared with γ-GDY.[28] The abundant ring-like diacetylenic linkages are ready to form carbon–metal bond with transition metals.[30–32] These features

J. Q. Li, Prof. Y. Xiong, Prof. C. G. Chen
School of Chemistry
and Chemical Engineering
Chongqing University
Chongqing 401331, P. R. China
Z. Q. Xie, Z. Z. Li, S. Q. Zhang, J. Y. Zhou, R. Liu, X. Gao, Prof. L. M. Tong, Prof. J. Zhang, Prof. Z. F. Liu
Center for Nanochemistry
Beijing Science and Engineering Center for Nanocarbons
Beijing National Laboratory for Molecular Sciences
College of Chemistry and Molecular Engineering
Peking University
Beijing 100871, P. R. China
E-mail: tonglm@pku.edu.cn; jinzhang@pku.edu.cn; zfliu@pku.edu.cn
Z. Z. Li, S. Q. Zhang, J. Y. Zhou, R. Liu
Academy for Advanced Interdisciplinary Studies
Peking University
Beijing 100871, P. R. China
Q. X. Huang
The National Center for Nanoscience and Technology
Beijing 100190, P. R. China

DOI: 10.1002/adma.201700421

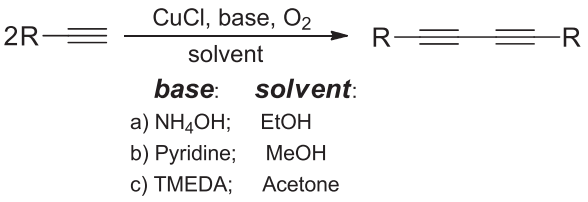

Scheme 1. The Glaser–Hay coupling reaction.[33–35] TMEDA = *N,N,N′,N′*-tetramethylethylenediamine.

make β-GDY a promising material for electron transportation and charge separation, which could be used in photocatalytic applications. Therefore, developing an approach to synthesize β-GDY and investigating its intrinsic properties and potential applications are highly desirable. However, there has been no available method to prepare β-GDY due to the complicated synthesis of precursors.

In this study, we present a feasible synthetic route to prepare β-GDY-containing thin film on copper foil with thickness about 25 nm using tetraethynylethene (TEE) as the precursor. Our synthetic strategy was derived from the Glaser–Hay coupling reaction that provides an efficient procedure for preparing symmetric diyne compounds in relatively high yields (**Scheme 1**).[33–35] The schematic illustration of synthetic strategy is depicted in **Figure 1**. First, TEE was prepared and used immediately from tetra[(trimethylsilyl)ethynyl]ethene (TEE-TMS) which was synthesized according to previous reported work.[36] Then, the monomer TEE was added into a three-neck flask containing acetone, pyridine, *N,N,N′,N′*-tetramethylethylenediamine (TMEDA), and pretreated copper foils. The four terminal alkyls on TEE have high reactivity and are easily coupled with each other to form an uniform carbon network structure. Taking into account the volatile property of TEE, we adopted a modified Glaser–Hay coupling reaction to synthesize the β-GDY-containing network structure.[33–35,37] In this process, the copper foil plays the roles of both a substrate and the source of catalyst,[38,39] where a Glaser–Hay reaction took place efficiently with the aid of organic base. As a result, a carbon film of 25 nm thickness on the surface of copper foil was obtained. Electrical measurement of the film showed the conductivity of 3.47×10^{-6} S m^{-1}. This film could be used as a metal-free electron transfer layer to fabricate TiO_2@β-GDY composite which greatly enhanced the photocatalytic activity of TiO_2.

The bonding structure and the elementary composition of β-GDY were studied systemically by Raman spectroscopy, Fourier transform infrared spectroscopy (FT-IR), X-ray photoelectron spectroscopy (XPS), and UV–vis absorption spectroscopy. **Figure 2**a shows typical Raman spectrum of β-GDY. As shown in the Raman spectrum, four dominant peaks appeared at 1460.1, 1577.1, 1902.8, and 2173.1 cm^{-1}, respectively. The peak at 1460.1 cm^{-1} comes from the vibration of carbon–carbon double bond that is consistent to the theoretical calculation.[40] The peak at 1577.1 cm^{-1} comes from the stretching vibration of sp^2 carbon domains in aromatic rings. The peak at 2173.1 cm^{-1} can be attributed to the stretching vibration of conjugated diyne links (−C≡C−C≡C−).[9,37] The Raman peak of diyne linkage presents an obvious hypochromatic shift compared to the Raman peak of monomer (Figure S2, Supporting Information), that is consistent with theoretical predictions (Figure S3, Supporting Information). The peak at 1902 cm^{-1} could be assigned to carbon–carbon triple bond according to previous works.[9,37] We note that no obvious changes of the β-GDY film were observed during the Raman spectroscopy characterization by 514 nm laser (0.09 mW) for 20 s, indicating the good stability of the synthesized β-GDY in air. FT-IR spectrum of as-grown GDY film on copper foil was displayed in Figure 2b. The band observed at 1060 cm^{-1} could be attributed to the stretching vibration of carbon–oxygen bond. The band of 2191 cm^{-1} is the typical carbon–carbon triple bone stretching vibration, that is in agreement with the result of Raman spectrum.[41]

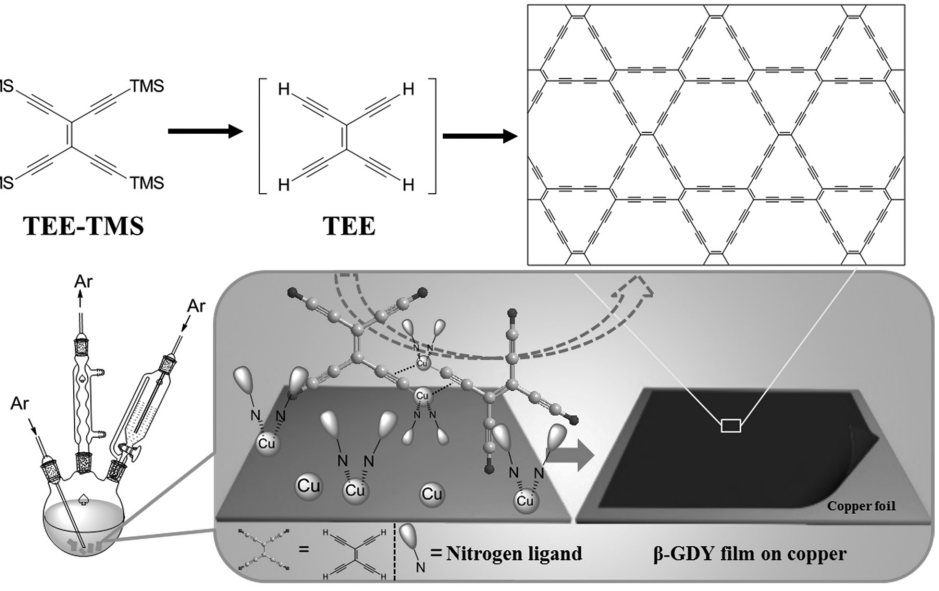

Figure 1. Schematic illustration of the experimental setup for the β-GDY-containing film growth on copper substrate.

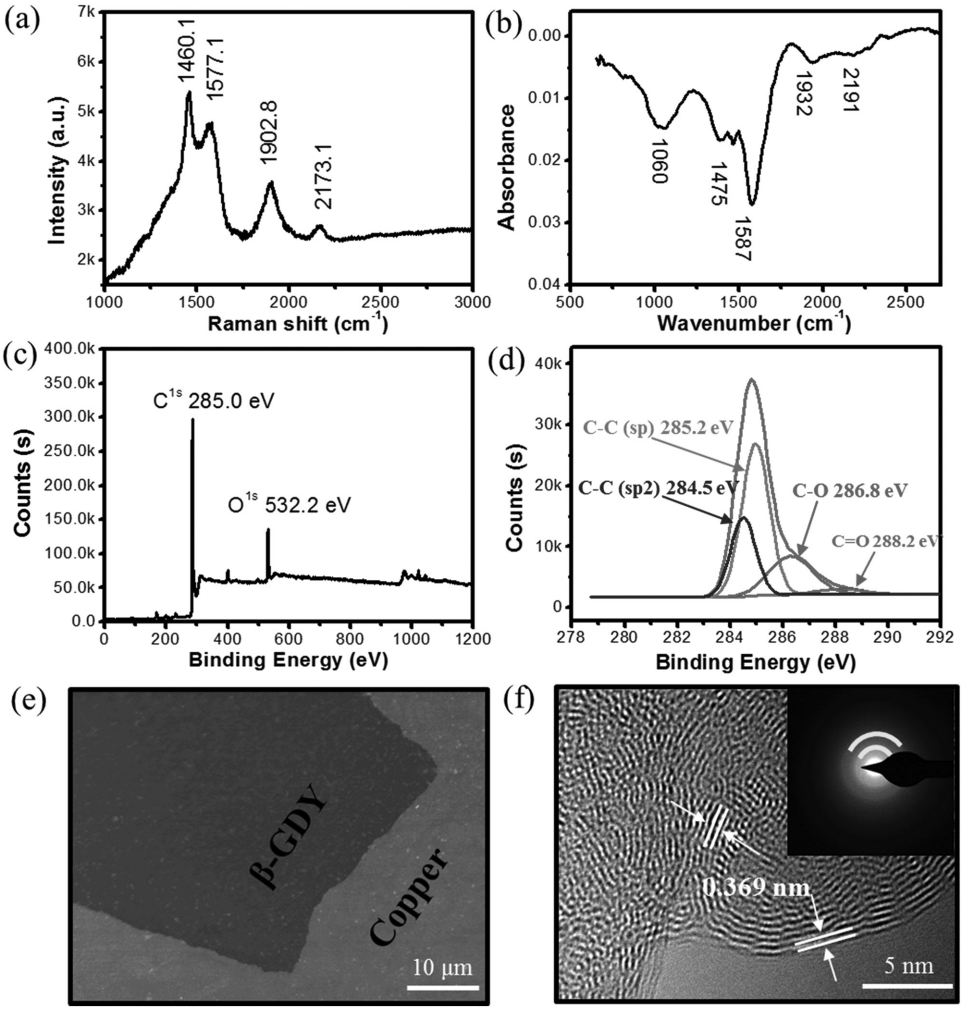

Figure 2. a) Raman spectrum of β-GDY film. b) FTIR spectrum of β-GDY film on copper foil. XPS spectra of β-GDY film: c) survey scan, d) narrow scan for element C1s. e) The SEM image of β-GDY film on copper substrate. f) HRTEM image of β-GDY; corresponding SAED pattern is shown in the inset.

XPS measurements indicated that the GDY is mainly composed of carbon element (Figure 2c). The existence of oxygen might result from the absorption of oxygen from air or the inevitable defects. Energy-dispersive spectrum results further confirmed the nearly pure carbon element (Figure S4a, Supporting Information). The peak at 285.0 eV shows essentially identical binding energy for the C1s orbital that can be deconvoluted into four subpeaks at 284.5, 285.3, 286.8, and 288.2 eV that are assigned to the C1s orbital of C=C, C≡C, C−O, and C=O bonds, respectively (Figure 2d). UV–vis absorption spectroscopy was also used to investigate the optical properties of as-prepared γ-GDY film (Figure S4b, Supporting Information). According to the UV–vis absorption measurements, there is an obvious bathochromic shift in the UV–vis spectra of the as-grown sample compared to monomers, which indicates that the extendedly conjugated π system formed due to alkynyl coupling enhanced electron delocalization.[37,42]

The morphology of the as-prepared β-GDY film was characterized by scanning electron microscopy (SEM). Figure 2e is a high magnification image of β-GDY film that displays the margin between β-GDY film and copper foil, which means that the copper substrate was uniformly covered by β-GDY film. Low magnification images of β-GDY film on a copper substrate (Figure S5, Supporting Information) show that the carbon film has a smooth surface and is continuous. Transmission electron microscopy (TEM) image indicates the layer-like structure of as-obtained β-GDY film (Figure S6, Supporting Information). High-resolution TEM (HRTEM) characterization clearly reveals curved streaks with a lattice parameter of 0.369 nm, which could be assigned to the interlayer distance of β-GDY (Figure 2f).[43] Corresponding selected area electron diffraction (SAED) pattern was shown in the inset of Figure 2f and its intensity integrating over 360° was also presented in Figure S6b (Supporting Information). This value is slightly higher than that of graphene owing to a more delocalized system of GDY and is close to that of γ-GDY.[13,44]

Atomic force microscopy (AFM) characterization of β-GDY film on SiO_2 plate indicates that the film has a smooth surface with a roughness about 2 nm and the thickness is about 25 nm (**Figure 3**a). The electrical properties of the β-GDY films on substrate were measured by peak force tunneling AFM, a variant of AFM using a conductive cantilever tip, which could indicate

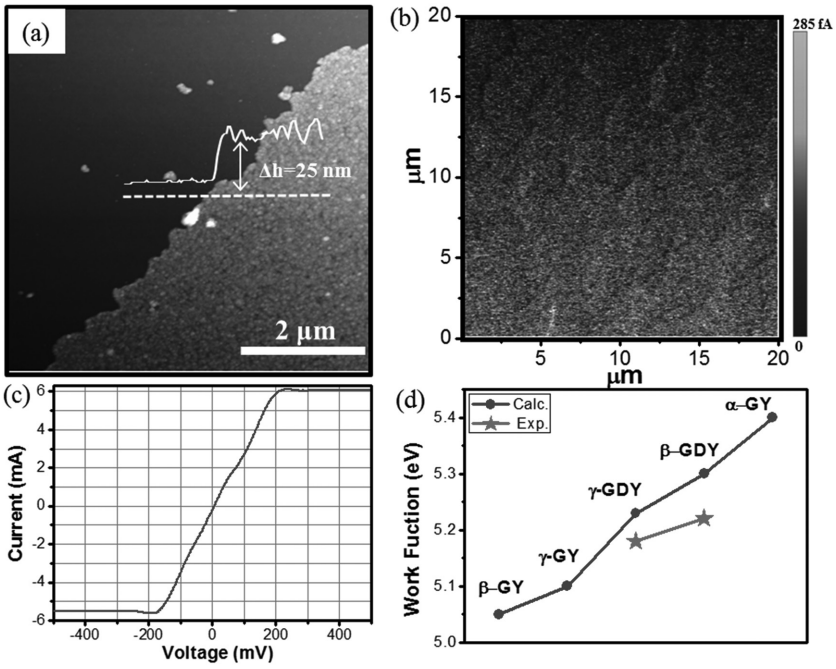

Figure 3. a) AFM image of β-GDY film transferred onto Si/SiO_2 substrate. b) Current AFM image. c) *I–V* curve of β-GDY film. d) Work functions of GY and GDY from theoretical predications and experimental measurements.

the current–voltage (*I–V*) characteristics as well as the surface contour of potential difference of the β-GDY film (Figure 3b). The *I–V* curves were measured on more than 100 sites at a bias voltage from –0.500 to +0.500 V. As shown in Figure 3c, the *I–V* relationship is highly linear in the voltage range between –0.200 and +0.200 V, which suggests the Ohmic behavior of β-GDY film. The conductivity was calculated as 3.47×10^{-6} S m^{-1}, indicating that the as-grown β-GDY is conductive, similar to γ-GDY.[9] To further explore the properties of β-GDY, the work functions were also investigated with Kelvin probe force microscopy using Pt–Ir-coated tip (Pt–Ir Φ = 4.86 eV) in ambient conditions and are shown in Figure 3d. The value of 5.22 eV of β-GDY is slightly higher than that of γ-GDY (Φ = 5.20 eV), which suggests the existence of alkyne-rich framework in β-GDY. For further proof of alkyne-rich architecture in β-GDY, we calculated the work functions of several GY family materials including α-, β-, and γ-GY or GDY (Table S1, Supporting Information). On account of high electron density around carbon–carbon triple bond, the higher percentage of alkyne in structure is and the stronger electrostatic potential in the material exists.

In terms of structure, β-GDY has a higher percentage of acetylenic linkages than that of γ-GDY, and has strong π-conjugation as γ-GDY. Moreover, β-GDY owns a conductive property because of its metallic behavior according to the theoretical predication.[15] These advantages imply that β-GDY might be of potential use in the fields of photocatalysis and photovoltaics. Previous reports have revealed that TiO_2@γ-GDY nanocomposite presented a higher photocatalytic activity compared to pure TiO_2.[45,46] Theoretical analysis demonstrated that Ti—C π bond is formed in TiO_2(001)@γ-GD composite because the high π-conjugation system of γ-GDY would make TiO_2 anchor to the GDY layer tightly and is beneficial for the charge transfer. Considering the highly π-conjugated system and the conductive property of the synthesized β-GDY-containing film, we applied it as an electronic transfer layer to enhance the photocatalytic performance of TiO_2. TiO_2@β-GDY composite was prepared through hydrothermal method. Its photocatalytic activity was evaluated by the degradation of organic dye methylene blue (MB). For comparison, TiO_2@γ-GDY was also prepared using the same method.

Figure 4a is the diagram of the catalytic processing. Briefly, electron–hole pairs were primarily formed on the semiconductor surface under light irradiation. β-GDY-containing film was used as an electron acceptor to prevent the electron–hole recombination of TiO_2. The holes were with high oxidability that can degrade

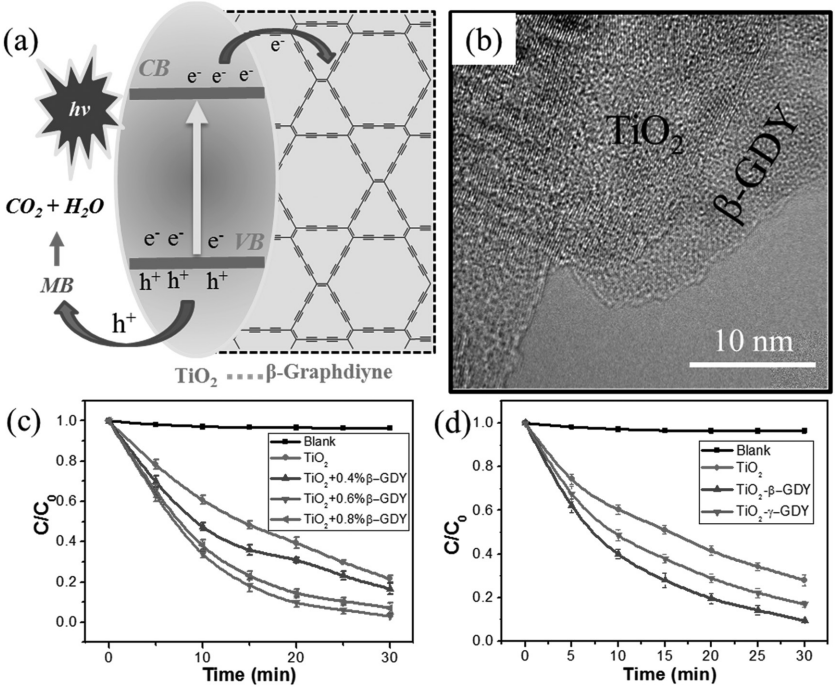

Figure 4. a) Schematic structure of TiO_2@β-GDY and tentative processes of the photodegradation of methylene blue (MB). b) HRTEM image of TiO_2@β-GDY. c) Photocatalytic degradation of MB over TiO_2 and different loading amount of β-GDY. d) Photocatalytic degradation of MB over TiO_2, TiO_2@γ-GDY, and TiO_2@β-GDY.

organic dye into carbon dioxide, water, or other products after several steps. The XPS survey spectra of the TiO_2@β-GDY composite indicated the presence of C1s, Ti2p, and O1s groups at binding energies 285, 459, and 530 eV, respectively (Figure S7a, Supporting Information). The C1s spectrum (Figure S7b, Supporting Information) can be deconvoluted into C—Ti, C—C (sp^2), C—C (sp), and C=O, and at binding energies 284.3, 284.7, 285.8, and 288.2 eV, respectively. Notably, the Ti—C bond at 284.3 eV was discerned, indicating the anchoring of TiO_2 on GDY layers that is beneficial to the electron transfer and would enhance the photocatalytic ability of TiO_2 according to previous work.[46] SEM and TEM images displayed the morphology characteristics of nanosheets and the SAED pattern could be indexed as [001] zone of TiO_2 (Figure S8a–c, Supporting Information). HRTEM image clearly showed the composition of TiO_2 and β-GDY (Figure 4b).[47] Moreover, the continuous atomic planes with a lattice spacing of 3.7 Å corresponding to the (100) planes of anatase TiO_2 single crystals were also shown (Figure S8d, Supporting Information).[48] The X-ray diffraction patterns and Raman spectrum of the products are shown in Figure S9 (Supporting Information).

The photocatalytic ability of TiO_2@β-GDY composite was evaluated by degrading MB under UV–visible light. According to the Beer–Lambert Law, the normalized temporal concentration change (C/C_0) of MB is proportional to the normalized maximum absorbance (A/A_0), which is used to investigate the degradation speed of MB. The blank test showed that the concentration of MB did not decrease without light irradiation. Bare TiO_2 owned a moderate catalytic ability for MB degradation. In order to optimize the photocatalytic ability of TiO_2@β-GDY, the composition ratio was controlled. As a result, TiO_2@β-GDY composites presented a superior photocatalytic efficiency than bare TiO_2, and the efficiency of different compositing ratio followed the order: 0.6 wt% > 0.8 wt% > 0.4 wt% of β-GDY (Figure 4c). For comparison, the optimized TiO_2@γ-GDY with 0.6 wt% carbon materials was also prepared and investigated (Figure 4d). The results showed that TiO_2@β-GDY had higher catalytic activity than TiO_2@γ-GDY composite and bare TiO_2. This is possibly due to the relative higher π-conjugated system in β-GDY that induced preferable synergistic effects between TiO_2 and β-GDY.[49,50] As mentioned above, the high π-conjugation system of GDY contributes to form of Ti—C π bond that is beneficial for the charge transfer. Compared to γ-GDY, the large ring-like frameworks of β-GDY provides a suitable coordination site for Ti atoms and the higher acetylenic linkages percentage of β-GDY (about 1.2 times to γ-GDY) would provide more Ti—C π bonds that can capture the photogenerated electrons from TiO_2 via a percolation mechanism. Hence, β-GDY acts as a preferable electron acceptor to suppress the charge recombination effectively, leaving more holes to form reactive species that promote the degradation of dyes.

In conclusion, we have developed a novel method to prepare β-GDY-containing thin film on copper foil using a modified Glaser–Hay coupling reaction where the copper foil acted as the roles of both a substrate and the source of catalyst. The synthesized film presented a smooth and uniform surface. The electronic property measurements of β-GDY film showed a conductivity of 3.47×10^{-6} S m^{-1} and a work function of 5.22 eV, which agreed well with theoretical calculations. In order to expand its application, we prepared TiO_2@β-GDY nanocomposite through hydrothermal process. In this composite, β-GDY played a role of electron transfer layer because of its conductive property and high π-conjugation system, and enhanced the photocatalytic performance of TiO_2.

Experimental Section

Synthesis of β-GDY-Containing Film: To a solution of 20 mg TEE-TMS and 10 mL tetrahydrofuran (THF) was added 0.2 mL tetrabutylammonium fluoride (TBAF) (1 M in THF) under argon atmosphere and stirred at 0 °C for 15 min. Then, the mixture was diluted with ethyl acetate, washed two times with saturated NaCl, dried by anhydrous $MgSO_4$, and filtered. The solvent was evaporated under vacuum while maintaining the temperature below 20 °C. The residue was diluted in 20 mL acetone and added dropwise for 10 h into a three-necked flask containing acetone (50 mL), pyridine (10 mL), TMEDA (2 mL), and copper foils. The reaction mixture was kept at 40 °C for 12 h under argon atmosphere. The entire process, from deprotection to addition, should be processed in dark, continuously, rapidly, and at low temperature to avoid decomposition of TEE. After completion of the reaction, the β-GDY-containing thin film was grown on copper foil and washed in turn with N, N-dimethyl formamide (DMF), acetone, and ethanol. Then, it was dried under N_2 flow.

Preparation of GDY Powder for the Synthesis of TiO_2@GDY Composites: β-GDY film was synthesized according to above procedures except that 40 mg TEE-TMS was used. Then, the copper foil was etched by 0.5 M $FeCl_3$ aqueous solution. The β-GDY film was collected and washed with 0.5 M HCl and deionized water repeatedly. Pure β-GDY powder was obtained after vacuum drying. γ-GDY powder was prepared using the similar method.

Photocatalytic Experiments: Photodegradation of MB was observed by using UV–vis absorption spectroscopy. In a typical process, 20 mg of photocatalyst was added into an aqueous solution of MB (0.01 g L^{-1}, 2.7×10^{-5} M, 40 mL) placed in a 50 mL cylindrical quartz vessel, ultrasonic dispersion before being stirred in the dark for 30 min. At given time intervals, the photoreacted solution was analyzed by recording variations of the absorption band maximum (663 nm) in the UV–vis spectra of MB. Under ambient conditions, 300 K recirculated water, and stirring, the photoreaction vessel was exposed to UV–visible light (λ > 300 nm) illumination (Xe lamp, 100 mW cm^{-2}). For detailed procedures of photocatalysts preparation, see the Supporting Information.

Supporting Information

Supporting Information is available from the Wiley Online Library or from the author.

Acknowledgements

J.Q.L. and Z.Q.X. contributed equally to this work. The authors thank Prof. Peng Gao for valuable discussions. This work was supported by the NSFC (21233001, 51432002, 51272006, and 21573004) and the MOST (2016YFA0200101 and 2016YFA0200104).

Received: January 21, 2017
Revised: February 13, 2017
Published online: March 15, 2017

[1] L. Dai, Y. Xue, L. Qu, H. Choi, J. Baek, *Chem. Rev.* **2015**, *115*, 4823.
[2] H. W. Kroto, J. R. Heath, S. C. O'Brien, R. F. Curl, R. E. Smalley, *Nature* **1985**, *318*, 162.

[3] S. Iijima, *Nature* **1991**, *354*, 56.
[4] K. S. Novoselov, A. K. Geim, S. V. Morozov, D. Jiang, Y. Zhang, S. V. Dubonos, I. V. Grigorieva, A. A. Firsov, *Science* **2004**, *306*, 666.
[5] R. H. Baughman, H. Eckhardt, M. Kertesz, *J. Chem. Phys.* **1987**, *87*, 6687.
[6] S. W. Cranford, M. J. Buehler, *Carbon* **2011**, *49*, 4111.
[7] A. L. Ivanovskii, *Prog. Solid State Chem.* **2013**, *41*, 1.
[8] A. R. Puigdollers, G. Alonso, P. Gamallo, *Carbon* **2016**, *96*, 879.
[9] G. Li, Y. Li, H. Liu, Y. Guo, Y. Li, D. Zhu, *Chem. Commun.* **2010**, *46*, 3256.
[10] S. Zhang, H. Liu, C. Huang, G. Cui, Y. Li, *Chem. Commun.* **2015**, *51*, 1834.
[11] Y. Guo, K. Jiang, B. Xu, Y. Xia, J. Yin, Z. Liu, *J. Phys. Chem. C* **2012**, *116*, 13837.
[12] K. Krishnamoorthy, S. Thangavel, J. Chelora Veetil, N. Raju, G. Venugopal, S. J. Kim, *Int. J. Hydrogen Energy* **2016**, *41*, 1672.
[13] C. Huang, S. Zhang, H. Liu, Y. Li, G. Cui, Y. Li, *Nano Energy* **2015**, *11*, 481.
[14] Z. Jin, M. Yuan, H. Li, H. Yang, Q. Zhou, H. Liu, X. Lan, M. Liu, J. Wang, E. H. Sargent, Y. Li, *Adv. Funct. Mater.* **2016**, *26*, 5284.
[15] J. Li, X. Gao, B. Liu, Q. Feng, X. Li, M. Huang, Z. Liu, J. Zhang, C. Tung, L. Wu, *J. Am. Chem. Soc.* **2016**, *138*, 3954.
[16] N. Yang, Y. Liu, H. Wen, Z. Tang, H. Zhao, Y. Li, D. Wang, *ACS Nano* **2013**, *7*, 1504.
[17] S. Wang, L. Yi, J. E. Halpert, X. Lai, Y. Liu, H. Cao, R. Yu, D. Wang, Y. Li, *Small* **2012**, *8*, 265.
[18] C. Kuang, G. Tang, T. Jiu, H. Yang, H. Liu, B. Li, W. Luo, X. Li, W. Zhang, F. Lu, J. Fang, Y. Li, *Nano Lett.* **2015**, *15*, 2756.
[19] S. Thangavel, K. Krishnamoorthy, V. Krishnaswamy, N. Raju, S. J. Kim, G. Venugopal, *J. Phys. Chem. C* **2015**, *119*, 22057.
[20] Z. Lin, *Carbon* **2016**, *108*, 343.
[21] R. Liu, H. Liu, Y. Li, Y. Yi, X. Shang, S. Zhang, X. Yu, S. Zhang, H. Cao, G. Zhang, *Nanoscale* **2014**, *6*, 11336.
[22] Z. Jin, Q. Zhou, Y. Chen, P. Mao, H. Li, H. Liu, J. Wang, Y. Li, *Adv. Mater.* **2016**, *28*, 3697.
[23] C. Wang, P. Yu, S. Guo, L. Mao, H. Liu, Y. Li, *Chem. Commun.* **2016**, *52*, 5629.
[24] X. Gao, J. Zhou, R. Du, Z. Xie, S. Deng, R. Liu, Z. Liu, J. Zhang, *Adv. Mater.* **2016**, *28*, 168.
[25] Y. Li, L. Xu, H. Liu, Y. Li, *Chem. Soc. Rev.* **2014**, *43*, 2572.
[26] W. Zhou, K. Chen, *Carbon* **2015**, *85*, 24.
[27] Z. Shao, Z. Sun, *Phys. E* **2015**, *74*, 438.
[28] J. Chen, J. Xi, D. Wang, Z. Shuai, *J. Phys. Chem. Lett.* **2013**, *4*, 1443.
[29] Z. Li, Z. Liu, Z. Liu, *Nano Res.* **2016**. DOI: 10.1007/s12274-016-1388-z.
[30] R. B. King, *Inorg. Chem.* **1968**, *7*, 1044.
[31] B. Demerseman, R. Mahe, P. H. Dixneuf, *J. Chem. Soc., Chem. Commun.* **1984**, 1394.
[32] Y. Obora, H. Moriya, M. Tokunaga, Y. Tsuji, *Chem. Commun.* **2003**, 2820.
[33] C. Glaser, *Ber. Dtsch. Chem. Ges.* **1869**, *2*, 422.
[34] G. Eglinton, A. R. Galbraith, *Chem. Ind.* **1956**, 737.
[35] A. S. Hay, *J. Org. Chem.* **1962**, *27*, 3320.
[36] J. Anthonyd, A. M. Boldia, Y. Rubin, M. Hobi, V. Gramlieha, C. B. Knobler, P. Seilerd, F. Diederich, *Helv. Chim. Acta* **1995**, *78*, 13.
[37] J. Zhou, X. Gao, R. Liu, Z. Xie, J. Yang, S. Zhang, G. Zhang, H. Liu, Y. Li, J. Zhang, Z. Liu, *J. Am. Chem. Soc.* **2015**, *137*, 7596.
[38] N. Hgbert, A. Beck, R. B. Lennox, G. Just, *J. Org. Chem.* **1992**, *57*, 1777.
[39] R. Bai, G. Zhang, H. Yi, Z. Huang, X. Qi, C. Liu, J. T. Miller, A. J. Kropf, E. E. Bunel, Y. Lan, A. Lei, *J. Am. Chem. Soc.* **2014**, *136*, 16760.
[40] P. Lambin, *Phys. Rev. B* **2013**, *88*, 75427.
[41] R. Dembinski, T. Bartik, B. Bartik, M. Jaeger, J. A. Gladysz, *J. Am. Chem. Soc.* **2000**, *122*, 810.
[42] M. Francoeur, M. P. Menguc, R. Vaillon, *Phys. Rev. B* **2011**, *84*, 75436.
[43] A. León, M. Pacheco, *Chem. Phys. Lett.* **2015**, *620*, 67.
[44] A. Reina, X. Jia, J. Ho, D. Nezich, H. Son, V. Bulovic, M. S. Dresselhaus, J. Kong, *Nano Lett.* **2009**, *9*, 30.
[45] S. Wang, L. Yi, J. E. Halpert, X. Lai, Y. Liu, H. Cao, R. Yu, D. Wang, Y. Li, *Small* **2012**, *8*, 265.
[46] N. Yang, Y. Liu, H. Wen, Z. Tang, H. Zhao, Y. Li, D. Wang, *ACS Nano* **2013**, *7*, 1504.
[47] G. Liu, H. G. Yang, X. Wang, L. Cheng, J. Pan, G. Q. M. Lu, H. Cheng, *J. Am. Chem. Soc.* **2009**, *131*, 12868.
[48] Q. Xiang, J. Yu, W. Wang, M. Jaroniec, *Chem. Commun.* **2011**, *47*, 6906.
[49] L. Zhang, H. Fu, Y. Zhu, *Adv. Funct. Mater.* **2008**, *18*, 2180.
[50] W. Wang, C. G. Silva, J. L. Faria, *Appl. Catal., B* **2007**, *70*, 470.